

Small Molecule Chemistry of the Pyrazolylborate–Zinc Unit $\text{Tp}^{\text{Cum,Me}}\text{Zn}$

Michael Ruf and Heinrich Vahrenkamp*

Institut für Anorganische und Analytische Chemie der Universität Freiburg, Albertstrasse 21, D-79104 Freiburg, Germany

Received March 28, 1996[⊗]

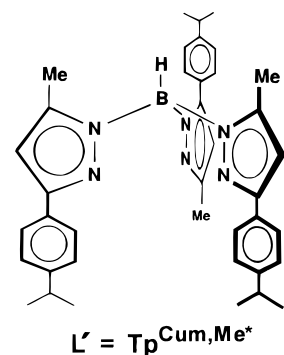
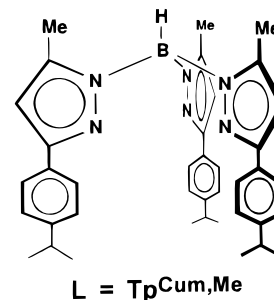
The synthesis of the highly encapsulating pyrazolylborate ligand hydrotris(3-*p*-cumenyl-5-methylpyrazolyl)borate ($\text{L} = \text{Tp}^{\text{Cum,Me}}$) and of its zinc hydroxide complex $\text{L}\cdot\text{Zn}-\text{OH}$ (**1**) are described. **1** is converted by H_2S into the hydrosulfide complex $\text{L}\cdot\text{Zn}-\text{SH}$ (**2**). Both **1** and **2** seem to be contaminated with traces of the isomeric species L' and $\text{2}'$ containing L' with one 3-methyl-5-*p*-cumenyl substituent. Thermal condensations of L' and **2** yield the molecular zinc oxide and sulfide complexes $\text{L}'\cdot\text{Zn}-\text{O}-\text{Zn}\cdot\text{L}'$ (**3'**) and $\text{L}'\cdot\text{Zn}-\text{S}-\text{Zn}\cdot\text{L}$ (**4**). The hydroxide complex **1** has been found to react readily with cumulated double-bonded species: CO_2 is incorporated in alcoholic solutions to form the alkylcarbonate complexes $\text{L}\cdot\text{Zn}-\text{OCOOR}$ (**5**). Similarly, CS_2 in ethanol forms the *O*-ethyl dithiocarbonate complex $\text{L}\cdot\text{Zn}-\text{SC}(\text{S})\text{OEt}$ (**6**). SO_2 is converted to a bridging sulfite ligand in $\text{L}\cdot\text{Zn}-\text{O}-\text{SO}-\text{O}-\text{Zn}\cdot\text{L}$ (**7**), and phenyl isothiocyanate is bound as a thiocarbamidato ligand in $\text{L}\cdot\text{Zn}-\text{SC}(\text{O})\text{NHPh}$ (**8**). Complexes **1**, **2**, **2'**, **3'**, **4**, **5**, and **6** have been confirmed by structure determinations and complexes **7** and **8** by spectral data.

Introduction

The introduction and splendid development of the hydrotris-(pyrazolyl)borate (Tp) ligands by Trofimenko and his partners^{1–3} have created a potential in classical coordination chemistry which can only be compared with that of the cyclopentadienyl ligands in organometallic chemistry. To our opinion the most unique aspect of this is the possibility to encapsulate metal ions by means of bulky substituents at the pyrazole 3-positions. This way low coordination numbers at the metals are enforced and cone angles beyond 250° are achieved.³ This is turn allows to attach labile ligand systems at the metals in the protective Tp pocket which in recent years has begun to be exploited in terms of $\text{TpM}-\text{X}$ complexes for unusual $\text{M}-\text{X}$ combinations^{4–7} or as bioinorganic model systems.^{8–10}

We have contributed to this in the field of zinc complexes, for simple $\text{TpZn}-\text{X}$ systems¹¹ as well as for a carbonic anhydrase enzyme model.¹² The Tp ligands used had phenyl or *tert*-butyl substituents at the pyrazole 3-positions ensuring the $\text{Zn}-\text{X}$ encapsulation and methyl substituents at the 5-positions to protect the B–N bonds against hydrolytic destruction. It became obvious that the 3-substituents used were still not optimal for the protection of some $\text{Zn}-\text{X}$ units, so that it was

desirable to increase their bulk. We chose to introduce the *p*-isopropylphenyl (*p*-cumenyl) substituents which subsequently turned out to be favorable not only for obtaining a stable and reactive $\text{TpZn}-\text{OH}$ complex¹³ but also for successfully encapsulating a large range of ligands X in $\text{TpZn}-\text{X}$. According to Trofimenko's nomenclature³ the resulting ligand is $\text{Tp}^{\text{Cum,Me}}$, being abbreviated here as **L** which in some cases was found to appear as its 3-methyl-5-cumenyl isomer L' .



This paper starts a series of full papers describing the zinc chemistry of ligand **L**. Preliminary reports have appeared on hydrolytic cleavages effected by $\text{L}\cdot\text{Zn}-\text{OH}$,¹³ on $(\text{L}\cdot\text{Zn})_2\text{O}$ and $(\text{L}\cdot\text{Zn})_2\text{S}$,¹⁴ and on the coordination of drug substances to the

[⊗] Abstract published in *Advance ACS Abstracts*, September 15, 1996.

- (1) Trofimenko, S. *Chem. Rev.* **1972**, *72*, 497–509.
- (2) Trofimenko, S. *Prog. Inorg. Chem.* **1986**, *34*, 115–210.
- (3) Trofimenko, S. *Chem. Rev.* **1993**, *93*, 943–980.
- (4) Han, R.; Parkin, G. *J. Am. Chem. Soc.* **1992**, *114*, 748–757.
- (5) Reinaud, O. M.; Yap, G. P. A.; Rheingold, A. L.; Theopold, K. *Angew. Chem.* **1995**, *107*, 2171–2173; *Angew. Chem., Int. Ed. Engl.* **1995**, *34*, 2051–2053.
- (6) Roberts, S. A.; Young, C. G.; Cleland, W. E.; Yamanouchi, K.; Ortega, R. B.; Enemark, J. H. *Inorg. Chem.* **1988**, *27*, 2647–2652.
- (7) Bucher, U. E.; Lengweiler, T.; Nanz, D.; von Philipsborn, W.; Venanzi, L. M. *Angew. Chem.* **1990**, *102*, 573–575; *Angew. Chem., Int. Ed. Engl.* **1990**, *29*, 548–549.
- (8) Kitajima, N.; Fujisawa, K.; Fujimoto, C.; Moro-oka, Y.; Hashimoto, S.; Kitagawa, T.; Toriumi, K.; Tatsumi, K.; Nakamura, A. *J. Am. Chem. Soc.* **1992**, *114*, 1277–1291.
- (9) Turowski, P. N.; Armstrong, W. H.; Roth, M. E.; Lippard, S. J. *J. Am. Chem. Soc.* **1990**, *112*, 681–690.
- (10) Looney, A.; Han, R.; McNeill, K.; Parkin, G. *J. Am. Chem. Soc.* **1993**, *115*, 4690–4697.
- (11) Alsfasser, R.; Powell, A. K.; Trofimenko, S.; Vahrenkamp, H. *Chem. Ber.* **1993**, *126*, 685–694.
- (12) Alsfasser, R.; Ruf, M.; Trofimenko, S.; Vahrenkamp, H. *Chem. Ber.* **1993**, *126*, 703–710.

(13) Ruf, M.; Weis, K.; Vahrenkamp, H. *J. Chem. Soc., Chem. Commun.* **1994**, 135–136.

(14) Ruf, M.; Vahrenkamp, H. *J. Chem. Soc., Dalton Trans.* **1995**, 1915–1916.

$L \cdot Zn$ unit.¹⁵ Here we will describe the synthesis of **L** and the central zinc complex $L \cdot Zn-OH$ as well as the reaction chemistry of the $L \cdot Zn$ unit with small molecule substrates.

Results and Discussion

Compounds KL and $L \cdot Zn-OH$ (1). The synthesis of ligand **L** required only small variations of the general procedure given by Trofimenko.¹⁶ Heating a melt of 3(5)-cumenyl-5(3)-methylpyrazole with KBH_4 to 240 °C produced the potassium salt **KL** which was obtained analytically pure by recrystallization from acetonitrile. **KL** has a good solubility in polar organic solvents and shows its typical B-H band in the IR at 2463 cm^{-1} . 1H -NMR spectra of **KL** indicated that the compound was not completely pure even after several recrystallizations. The most visible NMR signals of the "impurity" are weak peaks on the upfield sides of the aromatic signals of **KL**. Only after **2'** and **3'** (see below) had been structurally characterized it became evident that the impurity is the isomeric compound **KL'**. Such isomers of Tp ligands with bulky substituents have also been observed by Trofimenko.¹⁷ In our case the quantity of **L'**, as estimated from the NMR spectra or from the yields of **2'** and **3'**, must be 1% or less. We have not been able to enrich **KL'** or its zinc complex **1'** by chromatography or fractional crystallization, and thus the existence of **2'** and **3'** is the only indicator of their presence.

The conversion of **KL** into the hydroxide complex $L \cdot Zn-OH$ (**1**) is best achieved in dichloromethane/methanol using equimolar amounts of **KL**, $Zn(ClO_4)_2 \cdot 6H_2O$, and KOH. KOH serves the dual purpose of consuming one equivalent of acid from the intermediate $Zn-OH_2$ complex and precipitating all perchlorate. This allows the isolation of pure and crystalline **1** in good yields. **1** can also be obtained in methanol and without using KOH in a very slow reaction. Under these conditions, however, partial hydrolytic destruction of ligand **L** takes place, and the initial main product is the $H_3O_2^-$ bridged dinuclear cationic complex $[L \cdot Zn-OH \cdots H \cdots OH-Zn \cdot L]^+$. The chemistry of this complex which is one of the rare examples of $H_3O_2^-$ bridging and a model for oligonuclear hydrolytic zinc enzymes is reported in a different context.¹⁸

The isolated (i.e. not hydrogen-bridged) situation of the hydroxide ligand in **1** is evident from its sharp IR band at 3649 cm^{-1} which is near those of $Tp^{iBu,Me}Zn-OH$ ¹² and $Tp^{iPr,iPr}Zn-OH$.¹⁰ In contrast to the latter complexes, **1** did not allow the observation of a OH resonance in the 1H -NMR spectrum. The samples of **1** subjected to IR and NMR spectroscopy were solvent free powders. Crystalline **1** contains 1 equiv of methanol which is very easily lost. The crystals used for the structure determination therefore had to be handled in the presence of the mother liquor. They yielded the molecular structure of the hydrogen-bridged methanol solvate shown in Figure 1.

The coordination environment of zinc in **1** is trigonally distorted tetrahedral with Zn and O1 on the trigonal axis. The Zn-O bond (1.85 Å) is of the typical shortness of Zn-O bonds in this ligand environment^{11,12,15} and exactly matches that in $Tp^{iBu,Me}Zn-OH$.¹⁹ As Figure 1 shows, the OH ligand is buried well inside the hydrophobic pocket of the cumenyl substituents. This pocket can even encapsulate the methanol molecule which is hydrogen-bonded to the OH ligand. The X-ray data were

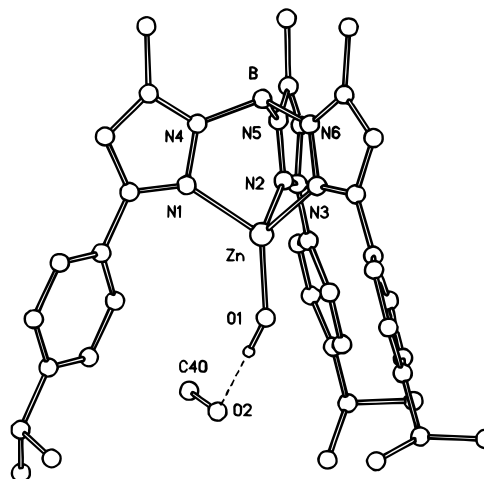


Figure 1. Molecular structure of **1**. Pertinent distances (Å): Zn-O1 1.847(4), Zn-N1 2.042(4), Zn-N2 2.039(4), Zn-N3 2.059(5), O1...O2 2.68(1). Bond angles (deg): O1-Zn-N1 125.8(2), O1-Zn-N2 122.2(2), O1-Zn-N3 121.1(2), N1-Zn-N2 94.5(2), N1-Zn-N3 91.5(2), N2-Zn-N3 93.2(2).

not good enough to decide whether the second H atom of the $CH_3-OH/Zn-OH$ adduct is located on O1 or on O2.

Complexes $L \cdot Zn-SH$ (2**) and $L' \cdot Zn-SH$ (**2'**).** Our studies of the complexes $Tp^{iBu,Me}Zn-OH$ ¹² and $Tp^{Ph,Me}Zn-OH$ ²⁰ had shown that their hydroxide ligand is an excellent leaving group. This is especially so when reagents leading to Zn-S bonds are offered. We had, however, not been able to introduce the SH ligand this way. Therefore the successful conversion of **1** into **2** was the proof for the superior stabilizing properties of **L**. Bubbling of H_2S through a solution of **1** in dichloromethane led to an almost quantitative yield of **2**. The contamination of **2** by **2'** going back to the contamination of **L** by **L'** was discovered accidentally when trying to obtain X-ray quality crystals from benzene. Under these conditions **2'** forms the more evenly shaped crystals, one of which was therefore picked. According to the visual impression the amount of **2'** was less than 1% of that of **2**. Good crystals of **2** were later obtained from acetonitrile.

2 and **2'** extend the still quite short list of metal-hydrosulfide complexes and are the first structurally characterized hydrosulfide complexes of zinc. **2** and **2'** could not be distinguished spectroscopically, and both do not show a typical SH absorption in the IR. They share this deficiency with other classical SH complexes,²¹ but not with organometallic ones.²² The complex $Tp^{iBu}Zn-SH$ which is related to **2** has recently been described in the literature.²³

The structures of **2** and **2'** (see Figures 2 and 3) show the typical ZnN_3X ligand distribution of the $TpZnX$ complexes. Compared to the structure of **1** the trigonal symmetry is somewhat distorted, as evidenced by the Zn-N bond lengths and S-Zn-N angles. Astonishingly the amount of distortion is the same in both complexes despite the significantly different environments of the sulfur atoms, and the Zn-SH unit in **2'** is stable even though the SH ligand is not fully encapsulated.

The Zn-S bond lengths in both complexes are practically identical. Their value (2.21 Å) corresponds to that in other $TpZn-SX$ complexes.¹¹ They are, however significantly shorter than in other tetrahedral complexes with Zn-S bonds.²⁴ Apart

(15) Hartmann, U.; Vahrenkamp, H. *Chem. Ber.* **1994**, *127*, 2381-2385.

(16) Trofimenko, S. *Inorg. Synth.* **1970**, *12*, 99-107.

(17) Rheingold, A.; White, C. B.; Trofimenko, S. *Inorg. Chem.* **1993**, *32*, 3471-3477.

(18) Ruf, M.; Weis, K.; Vahrenkamp, H. *J. Am. Chem. Soc.*, in press.

(19) Alsfasser, R.; Trofimenko, S.; Looney, A.; Parkin, G.; Vahrenkamp, H. *Inorg. Chem.* **1991**, *30*, 4098-4100.

(20) Ruf, M.; Weis, K.; Vahrenkamp, H. Unpublished work.

(21) DiVaira, M.; Midollini, A.; Sacconi, S. *Inorg. Chem.* **1977**, *16*, 1518-1524.

(22) Küllmer, V.; Vahrenkamp, H. *Chem. Ber.* **1976**, *109*, 1560-1568.

(23) Looney, A.; Han, R.; Gorell, I. B.; Cornebise, M.; Joon, K.; Parkin, G.; Rheingold, A. L. *Organometallics* **1995**, *14*, 274-288.

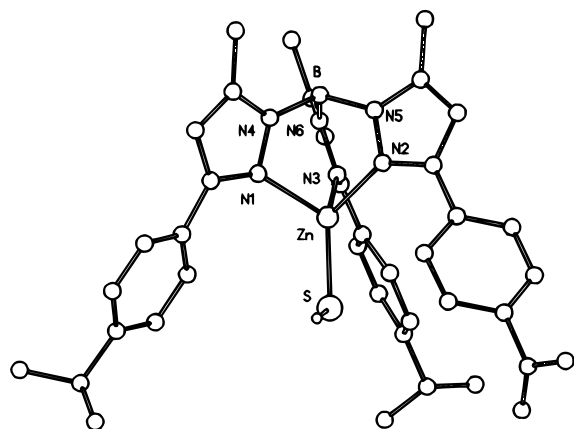


Figure 2. Molecular structure of **2**. Pertinent bond lengths (Å): Zn–S 2.210(3), Zn–N1 2.051(6), Zn–N2 2.072(6), Zn–N3 2.062(7). Bond angles (deg): S–Zn–N1 119.5(2), S–Zn–N2 123.5(2), S–Zn–N3 127.9(2), N1–Zn–N2 94.1(2), N1–Zn–N3 93.0(2), N2–Zn–N3 89.8(2).

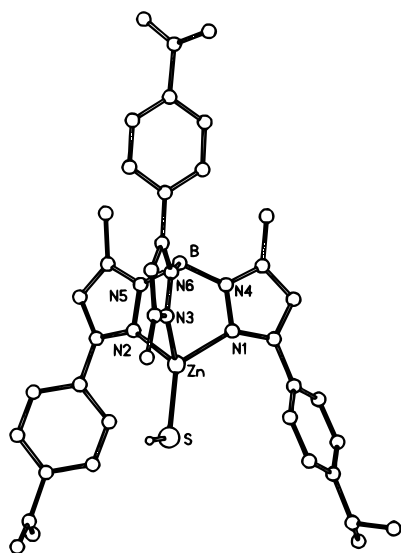


Figure 3. Molecular structure of **2'**. Pertinent bond lengths (Å): Zn–S 2.209(3), Zn–N1 2.037(7), Zn–N2 2.070(7), Zn–N3 2.058(7). Bond angles (deg): S–Zn–N1 129.0(2), S–Zn–N2 124.0(2), S–Zn–N3 118.5(2), N1–Zn–N2 90.5(3), N1–Zn–N3 92.8(3), N2–Zn–N3 92.5(3).

from the overall similarity of the molecules this relative shortening of the Zn–X bonds is a common feature of complexes **1** and **2**. It remains to be investigated whether the similar bonding pattern of **1** and **2** manifests itself also in similar reactivities.

Molecular Chalcogenides (L'·Zn)₂O (3') and (L'·Zn)₂S (4). The only evidence so far for similar reaction patterns of **1** and **2** was again found accidentally due to the contamination of **L** by **L'**. While this did not manifest itself in the discovery of **1'**, the existence of **1'** must be invoked to explain the formation of the dinuclear complex **3'**. **3'** was isolated from the last crystal fractions of **1** after prolonged times of reaction and handling. The simplest description of its formation consists in a thermal condensation of two molecules of **1'** which seems to be possible at or slightly above room temperature. The yield of **3'** was again less than 1%, but it was sufficient for a complete characterization, and the formation was reproducible.

The sulfur-bridged complex **4** was cleanly accessible by thermal treatment of **2**. At 200 °C the conversion took only a

few minutes. Evidence for the isomer **4'** was not found, and vice versa attempts to convert **1** thermally to **3** were unsuccessful. An alternative synthesis of **4** was found upon thermal treatment of the dithiocarbonate complex **6** (see below). **6** was heated with the intention to subject it to a Cugaev elimination²⁵ which under mild conditions liberates COS and ethylene, hoping to convert it to **2**. The gas evolution from **6**, however, started only above 190 °C at which temperature the expected **2** is transformed to **4**.

Complexes **3'** and **4** belong to the relatively small group of transition metal compounds having non-oligomeric molecular M–O–M or M–S–M units. There is some precedence for this in iron (Fe–O–Fe)²⁶ and, for a few cases, in molybdenum (Mo–S–Mo) chemistry,²⁷ but we have found only one other such pair of compounds for which both structures have been determined, viz. (salen)Fe–X–Fe(salen) with X = O²⁸ and S.²⁹ In zinc chemistry two-coordinate oxygen and sulfur are unprecedented.

The dinuclear nature of **3'** and **4** could be deduced from a feature of high diagnostic value in their ¹H-NMR spectra, namely the strong high-field shifts (0.5–1 ppm) for the cumenyl protons in comparison to those of the mononuclear complexes **1** and **2** (see Experimental Section). This results from the intertwining of the aromatic substituents from opposing Tp ligands in **3'** and **4** which exposes them mutually to their high-field shift ring current effects. This phenomenon is observed consistently for all dinuclear zinc complexes of aromatically substituted Tp ligands.

The inspection of the molecular structures of **3'** and **4** (see Figures 4 and 5) reveals that the general features of their TpZn–X units (Zn–O, Zn–S, and Zn–N bond lengths and general angle distribution) resemble those in the precursor complexes **1** and **2** and thus deserve no further comment. Some structural details show, however, that there is intramolecular crowding, especially in **4**. The most obvious of these are the occurrence of three untypically long Zn–N bonds and two unusually large N–Zn–N angles in **4**. As Figure 5 shows, these latter two angles involve the nitrogen atoms N1 and N103 which due to the bent Zn–S–Zn arrangement have the shortest N···N distance and hence the strongest interpenetration of their adjacent cumenyl substituents. This intramolecular steric crowding can explain the unusually large Zn–S–Zn angle in **4** (see below) and the nonexistence of **3**. In a hypothetical **3** the interligand repulsion would be even stronger due to the shorter Zn···Zn distance (3.7 vs 4.1 Å in **4**). Thus the unsymmetrical isomer **3'** is the only stable alternative, and its even distribution of Zn–N bond lengths and S–Zn–N angles indicates that it is relatively strain-free.

The most noticeable features of **3'** and **4** are their Zn–O–Zn and Zn–S–Zn angles of 180 and 139°, respectively. The value of 180° for **3'** is somewhat doubtful as the oxygen atom is located on an inversion center and displays very high anisotropy (see Figure 4). It cannot be much smaller than 180°, though. This results first from the overall molecular symmetry, i.e. the uniformity of the Zn–N bond lengths and O–Zn–N angles and the low anisotropy at the Zn and N atoms. Second, attempts to refine a structural model with disordered oxygen

(24) Brand, U.; Vahrenkamp, H. *Inorg. Chem.* **1995**, *34*, 3285–3293; *Chem. Ber.* **1996**, *129*, 435–440 and references cited therein.

(25) Nace, H. R. *Org. React.* **1962**, *12*, 57–100.

(26) Murray, K. S. *Coord. Chem. Rev.* **1974**, *12*, 1–35.

(27) Stiefel, E. In *Comprehensive Coordinations Chemistry*; Wilkinson, G., Gillard, R. D., McCleverty, J. A., Eds.; Pergamon: Oxford, England, 1987; Vol. 3, pp 1408–1412.

(28) Davies, J. E.; Gatehouse, B. M. *Acta Crystallogr., Sect. B* **1973**, *29*, 1934–1942.

(29) Dorfman, J. R.; Girerd, J. J.; Simhon, E. D.; Stack, T. D. P.; Holm, R. H. *Inorg. Chem.* **1984**, *23*, 4407–4412.

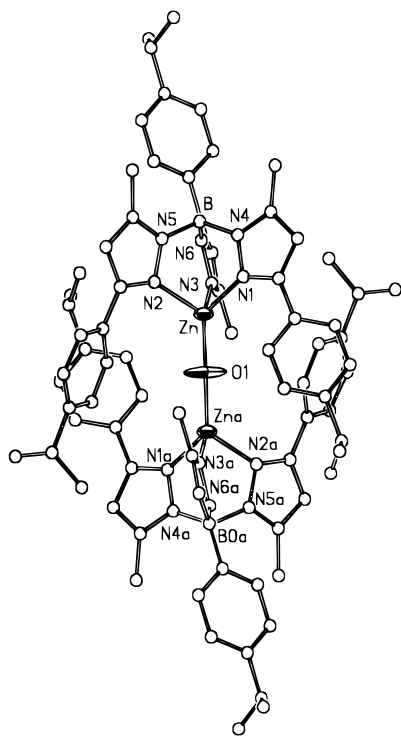


Figure 4. Molecular structure of **3'** displayed with thermal ellipsoids for Zn and O. Pertinent bond lengths (Å): Zn–O 1.854(1), Zn–N1 2.043(8), Zn–N2 2.014(8), Zn–N3 2.012(8). Bond angles (deg): O–Zn–N1 124.8(2), O–Zn–N2 122.0(2), O–Zn–N3 118.0(2), N1–Zn–N2 94.5(3), N1–Zn–N3 93.6(3), N2–Zn–N3 97.1(3), Zn–O–Zn 180.

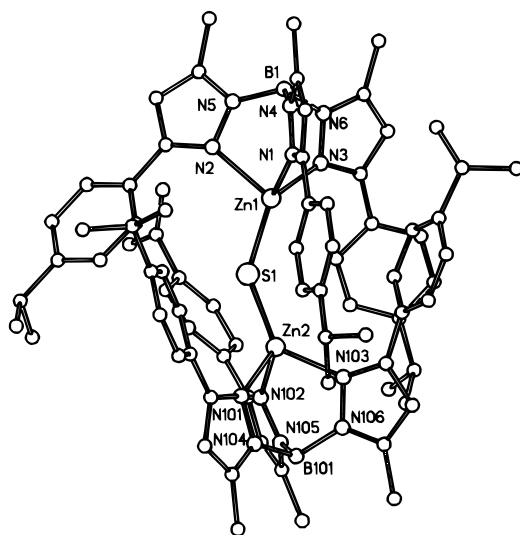


Figure 5. Molecular structure of **4**. Pertinent bond lengths (Å): Zn1–S 2.186(2), Zn2–S 2.189(2), Zn1–N1 2.099(5), Zn1–N2 2.183(5), Zn1–N3 2.088(5), Zn2–N101 2.141(6), Zn2–N102 2.142(5), Zn2–N103 2.066(5). Bond angles (deg): S–Zn1–N1 133.5(2), S–Zn1–N2 112.5(2), S–Zn1–N3 124.6(2), N1–Zn1–N2 90.5(2), N1–Zn1–N3 92.3(2), N2–Zn1–N3 92.5(2), S–Zn2–N101 123.8(2), S–Zn2–N102 111.2(2), S–Zn2–N103 136.3(2), N101–Zn2–N102 89.6(2), N101–Zn2–N103 88.9(2), N102–Zn2–N103 95.5(2), Zn1–S–Zn2 138.9(1).

atoms produced Zn–O–Zn angles not smaller than 172° and increased the *R* value by 0.6%.

Both Zn–X–Zn angles are unusually large albeit not totally out of range. Thus M–O–M angles of 180° are common in iron chemistry,²⁶ and the complex [Cp(CO)₃W]₂S displays a W–S–W angle of 127°.³⁰ In the only other pair of comparable complexes, [(salen)Fe]₂X^{28,29} the Fe–O–Fe and Fe–S–Fe

angles are 145 and 122°, respectively. In terms of modern molecular orbital calculations which have been applied in detail to main group element combinations like Si–O–Si and Si–S–Si,^{31,32} larger valence angles reflect higher bond polarities and a higher tendency for sp hybridization by oxygen. Accordingly the electronic nature of **3'** and **4** can be described in terms of strongly polar, but covalently bonded Zn–O–Zn and Zn–S–Zn units. The higher polarity allows or favors the linear Zn–O–Zn arrangement in **3'** irrespective of the steric requirements of the Tp ligands, and analogously the bent Zn–S–Zn arrangement in **4** is enforced by electronic reasons despite the steric strain.

Alkyl Carbonates L·Zn–OCOOR (R = Me, 5a; R = Et (5b)). It was to be expected that the molecular hydroxide **1** like its predecessors is a strong nucleophile capable of attacking acid anhydrides and hydrolyzable substrates and that its protective Tp ligand pocket stabilizes the products of nucleophilic attack. This has been verified to a large extent. The results of the small molecule reactions presented here also demonstrate that ligand **L** (Tp^{Cum,Me}) induces different reaction courses than other Tp ligands, for instance Tp^{tBu,Me}. As a rule, ligand **L** causes a higher reactivity of the Zn–OH function and a higher stability of the resulting Zn–X species, thereby enabling reactions which did not occur before.

The reactions between **1** and CO₂ can serve as an example for this. The analogous complex Tp^{tBu,Me}Zn–OH reacts with excess CO₂ in alcoholic solution forming unstable species, one of which presumably contains the Zn–OCO₂H unit and which upon blowing the solvent away with CO₂ crystallizes as the dinuclear carbonate complex.¹² In contrast, **1** picks up CO₂ from the atmosphere in alcoholic solution like soluble metal hydroxides, and in a CO₂ atmosphere it incorporates CO₂ quantitatively. This is unusual, though not unprecedented in zinc chemistry.^{33–35} The only products being formed are the alkyl carbonate complexes **5a** (R = Me) and **5b** (R = Et), and our attempts to obtain the carbonate complex L·Zn–O–CO–O–Zn·L failed. This is reminiscent of similar reactions with cyclam–zinc complexes³³ but unlike the observations with other zinc–ligand systems.^{12,34,35}

Complexes **5** are identified by ¹³C-NMR resonances at 158 ppm for the carbonate carbon, by IR bands at 1715 and 1300 cm⁻¹ for the C–O stretches, and by ¹H-NMR resonances with strong high-field shifts for the alkoxy groups (see Experimental Section). The fact that 1 equiv of alcohol is incorporated in addition to CO₂ in **5a,b** may be related to a better stabilization of the COOR ester group rather than the COOH acid group in the hydrophobic Tp ligand pocket. In agreement with this complexes **5** are stable in alcohol/water mixtures with up to 20% water while the corresponding Tp^{tBu,Me}Zn–OCOOR complexes whose COOR group is not encapsulated are quite sensitive to water.¹²

The molecular structure of **5a** (see Figure 6) displays a strictly unidentate alkylcarbonate ligand similar to that in Tp^{tBu,Me}Zn–OCOOR.¹² This is obvious from the rather symmetrical OZnN₃ arrangement and the close to 120° angles at O1 and O2. There seem to be electronic reasons for this, as MO

(30) Kubas, G. J.; Wassermann, H. J.; Ryan, R. R. *Organometallics* **1985**, *4*, 419–421.

(31) Kutzelnigg, W. *Angew. Chem.* **1984**, *96*, 262–286; *Angew. Chem., Int. Ed. Engl.* **1984**, *23*, 272–295.

(32) Bock, H. *Angew. Chem.* **1989**, *101*, 1659–1682; *Angew. Chem., Int. Ed. Engl.* **1989**, *28*, 1627–1650.

(33) Kato, M.; Ito, T. *Inorg. Chem.* **1985**, *24*, 509–514.

(34) Murthy, N. N.; Karlin, K. D. *J. Chem. Soc., Chem. Commun.* **1993**, 1236–1238.

(35) Kitajima, N.; Hikichi, S.; Tanaka, M.; Moro-oka, Y. *J. Am. Chem. Soc.* **1993**, *115*, 5496–5508.

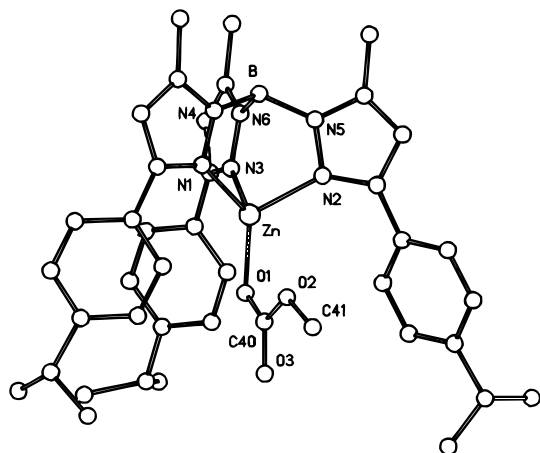


Figure 6. Molecular structure of **5a**. Pertinent bond lengths (Å): Zn–O1 1.924(4), Zn–N1 2.050(5), Zn–N2 2.011(4), Zn–N3 2.080(5), O1–C40 1.27(1), C40–O2 1.30(1), C40–O3 1.27(1). Bond angles (deg): O1–Zn–N1 126.9(2), O1–Zn–N2 121.4(2), O1–Zn–N3 117.8(2), N1–Zn–N2 97.9(2), N1–Zn–N3 91.6(2), N2–Zn–N3 92.8(2), Zn–O1–C40 118.7(5), O1–C40–O2 119.0(8), O1–C40–O3 123.4(9), O2–C40–O3 117.6(11), C40–O2–C41 123.6(10).

calculations on $\text{TpZn-OCO}_2\text{H}$ and TpZn-ONO_2 complexes have shown.³⁶ Crystal data of a CO_2 adduct of an inactivated mutant of the enzyme carbonic anhydrase indicate, however, that in the enzyme the bicarbonate ligand is coordinated in a bidentate fashion to the His_3Zn unit.³⁷ The Zn–O bond in **5a** is longer than that in $\text{Tp}^{\text{Bu,Me}}\text{Zn-OCOOMe}$ (1.88 Å¹²) but shorter than that in $[(\text{Me}_4[14]\text{aneN}_4)\text{Zn-OCOOMe}]\text{ClO}_4$ (1.97 Å³³). The planarity of the alkylcarbonate ligand, its uniform C–O bond lengths, and its complete set of near-to-120° angles qualify it as a delocalized system.

The O-Alkyl Dithiocarbonate $\text{L}\cdot\text{Zn-SC(S)OEt}$ (6**).** Carbon disulfide which previously had been found not to react with Zn–OH complexes was incorporated by **1** as easily as carbon dioxide. The course of the reaction was completely analogous to that of the CO_2 reaction, i.e. the additional incorporation of the solvent ethanol produced the *O*-ethyl dithiocarbonate complex **6**. As a result of this reaction, **6** was always accompanied by the dinuclear sulfide **4**, from which it was difficult to separate. This is puzzling as the thermal conversion $\text{6} \rightarrow \text{4}$ (see above) requires temperatures around 200 °C. It must therefore be assumed that a reaction intermediate, possibly $\text{L}\cdot\text{Zn-OCSSH}$ or $\text{L}\cdot\text{Zn-S-CO-S-Zn}\cdot\text{L}$, has a high tendency for COS elimination leaving **4** or a labile precursor thereof behind. Pure **6** could be obtained more conveniently and in high yields by reaction between **1** and potassium xanthogenate (KCS_2OEt).

Unlike for complexes **5** there is no strong spectroscopic evidence for the constitution of **6** except for the high-field ¹H-NMR resonances of the ethyl group. The structure determination (see Figure 7) therefore had to provide this evidence as well as some data for a comparison with the CO_2 derived complex **5a**.

The overall similarities between **5a** and **6** are obvious. They concern the rather symmetrical $\text{N}_3\text{Zn-X}$ environments, the monodentate attachment of the (thio)carbonate ligands, the point of attachment and orientation of the *O*-alkyl groups, the planarity of the whole (thio)carbonate ligands, and the elongation of the Zn–X bonds with respect to those in the corresponding Zn–XH complexes. Typical features of sulfur in **6** are the small

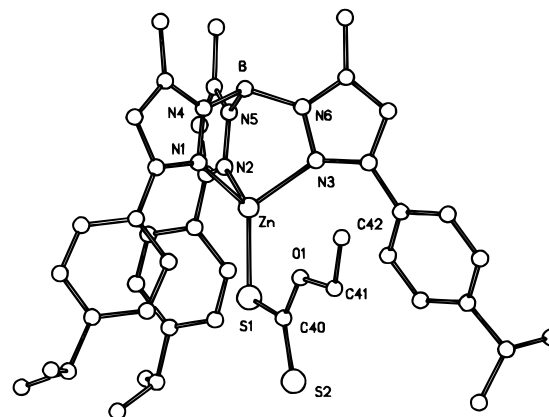


Figure 7. Molecular structure of **6**. Pertinent bond lengths (Å): Zn–S1 2.264(1), Zn–N1 2.055(3), Zn–N2 2.077(3), Zn–N3 2.052(2), S1–C40 1.726(4), C40–S2 1.642(4), C40–O1 1.337(4). Bond angles (deg): S1–Zn–N1 126.5(1), S1–Zn–N2 115.9(1), S1–Zn–N3 125.1(1), N1–Zn–N2 91.5(1), N1–Zn–N3 96.1(1), N2–Zn–N3 92.6(1), Zn–S1–C40 104.4(1), S1–C40–S2 122.3(2), S1–C40–O1 113.0(2), S2–C40–O1 124.8(3), C40–O1–C41 119.2(3).

valence angle at S1 and the lack of delocalization in the COS_2 triangle (cf. bond lengths). The comparison of **6** with other zinc–ethyl dithiocarbonate complexes^{38–40} reveals that **6** seems to be the cleanest case of monodentate coordination, whereas the reference compounds display intermediate stages between monodentate and bidentate, including bridging, coordination. **6** also has the shortest Zn–S distance for this type of ligands which may, however, be related to the fact that it is the only tetrahedral complex in the series.

Considering the large number of known *O*-alkyl dithiocarbonate complexes and the preference of zinc for sulfur donors, the existence of **6** is not surprising. Accordingly the novelty in its formation is the attack of the Zn–OH nucleophile on CS_2 , which differs from the standard sequence of metal *O*-alkyl dithiocarbonate formation by reaction between a metal alkoxide and CS_2 . This cannot be the case here since we have found that the alkoxides TpZn-OR are so sensitive toward traces of water that they don't persist in alcoholic solution, not to say in the presence of water liberated during the formation of **6**.

The μ -Sulfite Complex $\text{L}\cdot\text{Zn-O-SO-O-Zn}\cdot\text{L}$ (7**).** On the basis of the literature on reactions between metal aqua complexes and SO_2 ⁴¹ it was expected that nucleophilic attack of **1** on SO_2 would produce a terminal sulfite ligand labile toward isomerization or oxidation in a complex of low thermal stability. We were therefore surprised to find that the reaction produces the stable dinuclear complex **7** containing the dianionic SO_3^{2-} bridge, the analogue of which (CO_3^{2-}), again to our surprise, was not formed in the CO_2 reaction. **7** is formed quantitatively with a stoichiometric amount of SO_2 and destroyed upon bubbling SO_2 through the solution, because the solution becomes so acidic that ligand **L** is decomposed.

As X-ray quality crystals of **7** could not be obtained, its constitutional assignment rests on the spectra alone. Beside the elemental composition the ¹H-NMR data are the strongest indicator, displaying the typical high-field shifts for the cumenyl substituents (see Experimental Section) as observed and discussed for **3'** and **4**. Evidence for the given bridging type and

(36) Pavan Kumar, P. N. V.; Marynick, D. S. *Inorg. Chem.* **1993**, *32*, 1857–1859.

(37) Xue, Y.; Vidgren, J.; Svenson, L. A.; Liljas, A.; Jonsson, B. H.; Lindskog, S. *Proteins: Struct. Funct. Genet.* **1993**, *15*, 80–87.

(38) Raston, C. L.; White, A. H.; Winter, G. *Aust. J. Chem.* **1976**, *29*, 731–738.

(39) Ikeda, T.; Hagihara, H. *Acta Crystallogr.* **1966**, *21*, 919–927.

(40) Baggio, R.; Frigerio, A.; Halac, E. B.; Vega, D.; Pereg, M. *J. Chem. Soc., Dalton Trans.* **1992**, 1887–1892.

(41) Maragh, P. T.; Dasgupta, T. P.; Williams, D. J. *J. Chem. Soc., Dalton Trans.* **1995**, 2843–2849, and references cited therein.

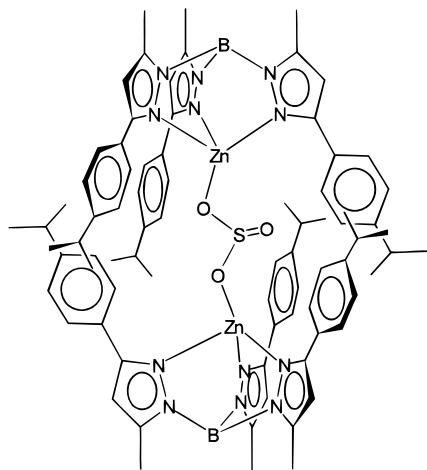


Figure 8. Proposed structure of complex 7.

the Zn–O coordination comes from the single medium-to-strong $\nu(\text{SO})$ IR band at 886 cm^{-1} , which is in the area typical for O-bonded sulfite ligands⁴² and near those of other sulfite–O-bridged first-row transition metal complexes.^{41,43} Furthermore a bridging arrangement like Zn–SO₂–O–Zn with one Zn–S and one Zn–O connection should give rise to two sets of NMR resonances for the Tp ligands. Thus the available evidence allows to propose the structure of **7** as shown in Figure 8.

As mentioned above, classical complexes with sulfite ligands are labile, being easily subjected to hydrolysis or oxidation, and sulfite O-bridged complexes are rare. In the light of this the stability of **7** is once more remarkable and must be related to the encapsulation of the central [Zn–SO₃–Zn]²⁺ unit by six cumenyl substituents again. Unlike the situation in **4** where the close proximity of the two Zn·L units creates steric strain, the more extended bridge in **7**, which should cause a Zn···Zn separation of about 5.5 Å, allows one to avoid the strain while still allowing the protective enclosure.

The Thiocarbamate Complex L·Zn–SC(O)NPh (8). The last cumulated double bond system showing reactivity toward **1** was phenyl isothiocyanate. While PhNCO did not react, PhNCS was quantitatively converted to complex **8**. The formation of **8** requires the isomerisation of an O-bonded intermediate which must be driven by the thiophilicity of zinc which is also responsible for the stability of **8**.

The constitution of **8** can be derived with some certainty from its spectra. The ¹H-NMR spectrum shows the presence of all constituents and gives no unusual signal shifts except for the relatively high location of the NPh resonances. The IR spectrum shows the NH stretch at 3232 cm^{-1} and an intense CO band at 1613 cm^{-1} , thereby leaving no doubt about the atom sequence in the thiocarbamate ligand. The resulting structural proposal is displayed in Figure 9.

Conclusions

The new pyrazolylborate ligand Tp^{Cum,Me} (**L**) has been shown to have a very high potential for confining a metal to a low coordination number while at the same time providing a protective pocket for one additional labile ligand unit. This property has been exploited here for the incorporation of very small labile units and for the reaction with small molecule substrates. As a result several new bonding types and new reactive systems have been found.

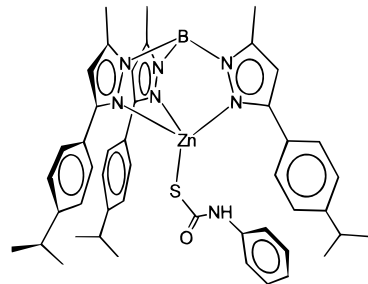


Figure 9. Proposed structure of complex 8.

The key to the successful exploitation of the L·Zn–X chemistry was the stability and ease of preparation of the hydroxide complex **1**. The very fact that **1** exists as such in aqueous methanol solution implies that the pK_a of the corresponding Zn–OH₂ complex is 7 or less, which means that **1** qualifies as a model for hydrolytic zinc enzymes. The chemically most useful consequence of this is the high nucleophilicity of the Zn–OH function which has been put to use here. The acid–base properties of **1** include the capacity for hydrogen bonding as has been observed in the structure of **1**·CH₃OH. They also yield one explanation for the fact that the OH function in **1** is a good leaving group being replaced by the anion X of most weak acids HX having a pK_a lower than 7;²⁰ i.e. the real leaving group is H₂O being produced by protonation.

A simple application of the leaving group concept was the formation of the SH complex **2** from **1** and H₂S. In this case the thiophilicity of zinc provides part of the driving force for the substitution and of the stability for the labile Zn–SH combination. While in most classical complexes M–SH combinations are unstable with respect to metal sulfide formation, complex **2** persists at temperatures up to 200 °C. But even then it does not lose its Tp ligand but manifests its tendency to move toward zinc sulfide in the formation of the Zn–S–Zn complex **4**.

The Zn–O–Zn and Zn–S–Zn complex **3'** and **4** are the most striking examples of the encapsulating power of the Tp^{Cum,Me} ligands. In **3'** and **4** the basis of all coordination chemistry (many donors per metal) is inverted for the bridging oxide and sulfide ligands. Thereby the L·Zn units are simple univalent substituents in a covalent OX₂ or SX₂ bonding situation, allowing a discussion of the factors determining valence angles at oxygen and sulfur.

The nucleophilicity of the Zn–OH unit in **1** was used here for the attack on cumulated double bond systems. In these reactions the first step is supposed to consist of the addition of the OH function across one double bond, as exemplified by the conversion of CO₂ to Zn–O–C(O)–OH. In all four cases investigated, the isolated products were due to a subsequent additional reaction. For the CO₂ and CS₂ incorporations the second reaction is an esterification of the coordinated carbonic acid by the alcohol solvent leading to complexes **5** and **6**. In the case of **6** a third reaction step exchanging the Zn–O for a Zn–S coordination must be invoked. The high tendency of formation of the alkyl carbonate complexes draws the attention to a potential practical application of zinc complexes like **1**, namely their use in catalytic conversions of CO₂.

The substrate SO₂ was the only one in this paper undergoing a reaction with 2 equiv of **1**. We assume that the first reaction step produces the bisulfite complex L·Zn–OSO₃H which behaves like an oxoacid toward the second molecule of **1**, expelling H₂O and generating the sulfite bridge in **7**. The resulting composition of **7** does not involve Zn–S bonds and therefore may remain disputed until its confirmation by a structure determination. In contrast, the proposed composition

(42) Nakamoto, K. *Infrared and Raman Spectra of Inorganic Coordination Compounds*, 3rd ed.; Wiley: New York, 1978.

(43) Wiegardt, K.; Druke, S.; Chaudhuri, P.; Flörke, V.; Haupt, H. J.; Nuber, B.; Weiss, J. *Z. Naturforsch., B* **1983**, *44*, 1093–1101.

of **8**, the product of the PhNCS reaction, seems to be undoubtable. In this case it is to be assumed again that the Zn–O-bonded reaction intermediate $L'Zn-OC(S)NHPH$ is isomerized to the Zn–S-bonded product **8**.

The reactions described here are the simplest of **1** and mark the beginning of the exploitation of its chemistry as well as that of its derivatives. Further simple acids like H_2S with OH, SH, and NH acidity and further double-bonded systems susceptible to nucleophilic attack like $S=C=X$, $N=S=X$, allene, and ketene come to mind. Also, nucleophilic substrate cleavages by the Zn–OH function are attractive on the background of bioinorganic model chemistry.

Several of the products obtained here are candidates themselves for a new reaction chemistry. One of them is the SH complex **2** which may have as rich a chemistry as **1**, another one the sulfite complex **7**. Above all the chemical behavior of the carbonate derivatives **5** is attractive to us. It will have to be tested whether their formation is reversible, whether they allow the attachment of a second substituent to the substrate CO_2 , and whether they open an entry to catalytic CO_2 reactions.

Experimental Section

General Data. All experimental techniques and the standard IR and NMR equipment were as described previously.⁴⁴ Starting materials were obtained commercially. Solvents were dried according to standard laboratory procedures. Unless otherwise stated, reactions were carried out in a water-free atmosphere, normally under nitrogen (99.99%). 3-(5-Cumenyl-5(3)-methylpyrazole)⁴⁵ was prepared starting from cumene via *p*-isopropylacetophenone⁴⁶ and cumenylacetone.⁴⁷

Preparations. $KTp^{Cum,Me}$ (KL). A 10.0 g (49.9 mmol) sample of 3(5)cumenyl-5(3)-methylpyrazole and 0.90 g (16.6 mmol) of KBH_4 were combined in a three-necked 250 mL flask equipped with an immersing thermometer, a stirrer, and a gas outlet. Within 2 h the temperature of the mixture was raised to 240 °C and the melt stirred until no more gas was evolved (ca. 1 h). After the melt was cooled to room temperature, the resulting glassy solid was broken up and the resulting powder extracted with 100 mL of boiling petroleum ether (60–70 °C) in order to remove any remaining pyrazole. The colorless residue was recrystallized from acetonitrile at –30 °C. After filtration and pumping to remove all solvent of crystallization 7.21 g (67%) of potassium hydrotris(3-cumenyl-5-methylpyrazolyl)borate (KL, $KTp^{Cum,Me}$) remained as a colorless powder, mp 123 °C, $\nu(BH)$ 2463 cm^{-1} . Anal. Calcd for $C_{39}H_{46}BKN_6$: C, 72.20; H, 7.15; N, 12.96. Found: C, 72.27; H, 7.10; N, 12.88.

$L'Zn-OH$ (1). A 1.00 g (1.54 mmol) sample of KL in 50 mL of dichloromethane was combined with 574 mg (1.54 mmol) of $Zn(ClO_4)_2 \cdot 6H_2O$ in 10 mL of methanol. After 2 h of stirring, 86 mg (1.54 mmol) of KOH powder was added. The mixture was stirred for another 15 h and filtered. Then 30 mL of methanol was added to the filtrate, the volume of which was then reduced to one-third in a rotary evaporator with a 40 °C water bath. From the remaining solution within a few hours 743 mg (70%) of colorless **1**, mp 205 °C, $\nu(BH)$ 2550 cm^{-1} , was precipitated, which was filtered off and dried in vacuo. Anal. Calcd for $C_{39}H_{47}BN_6OZn$: C, 67.69; H, 6.85; N, 12.15. Found: C, 67.23; H, 6.56; N, 11.92.

$L'Zn-SH$ (2) and $L'Zn-SH$ (2'). Hydrogen sulfide was bubbled for 15 min through a solution of 200 mg (0.29 mmol) of **1** in 30 mL of dichloromethane. Small amounts of a cloudy precipitate were removed by centrifugation. The solvent was removed in vacuo and the residue picked up in a minimum amount of acetonitrile. Cooling to –30 °C precipitated 186 mg (91%) of colorless **2**, $\nu(BH)$ 2547 cm^{-1} , which sublimates at 106 °C. During attempts to grow X-ray quality crystals from benzene, minute amounts of **2'** were discovered whose

crystals were more evenly shaped than those of **2**. Anal. Calcd for $C_{39}H_{46}BN_6SZn$: C, 66.15; H, 6.69; N, 11.87. Found: C, 66.73; H, 6.79; N, 11.88.

$(L'Zn)_2O$ (3'). Performing a double-sized run for the synthesis of **1** up to the first crystallization yielded 1.32 g (62%) of **1**. The mother liquor was again reduced in vacuo to yield another 210 mg (10%) of **1**. Then 5 mL of dichloromethane was added and the volume of the solution reduced in a stream of nitrogen to 2 mL. Then the remaining solvent was removed with a syringe and the crystalline residue dried in a stream of nitrogen. A 13 mg (0.6%) yield of colorless **3'**, mp 158 °C, $\nu(BH)$ 2553 cm^{-1} , remained. Anal. Calcd for $C_{78}H_{92}B_2N_{12}OZn_2 \cdot 2CH_2Cl_2$: C, 62.25; H, 6.31; N, 11.07; Zn 9.8. Found: C, 62.56; H, 6.30; N, 10.95; Zn, 8.5.

$(L'Zn)_2S$ (4). (a) **From 2.** A 200 mg (0.28 mmol) sample of **2** was quickly heated to 200 °C. The powdery starting material turned brown without melting. Immediately after, the product was allowed to cool to room temperature, washed twice with 5 mL of diethyl ether each, and recrystallized from benzene/methanol (1:2). A 162 mg (83%) yield of **4** resulted.

(b) **From 6.** 200 mg (0.25 mmol) of **6** were heated slowly to 200 °C. The complex started melting at 170 °C. At 190 °C some gas was evolved from the melt. After the melt was cooled to room temperature, a brownish impurity was removed by washing twice with 5 mL of diethyl ether each. Recrystallization from benzene/methanol (1:2) yielded 150 mg (83%) of **4**. **4** forms colorless crystals, mp 278 °C dec, $\nu(BH)$ 2544 cm^{-1} . Anal. Calcd for $C_{78}H_{92}B_2N_{12}SZn_2$: C, 67.78; H, 6.71; N, 12.16. Found: C, 67.76; H, 6.75; N, 12.09.

$L'Zn-OCOOME$ (5a). A 200 mg (0.29 mmol) sample of **1** was dissolved in 30 mL of dichloromethane, and 20 mL of methanol was added. A slow stream of CO_2 was passed through the solution for 10 min. The flask was placed in a desiccator charged with $CaCl_2$ and filled with CO_2 . After 5 days, 183 mg (84%) of colorless, crystalline **5a**, mp 240 °C dec, $\nu(BH)$ 2551 cm^{-1} , $\nu(CO)$ 1714 and 1294 cm^{-1} , had precipitated which was filtered off and dried in vacuo. Anal. Calcd for $C_{41}H_{49}BN_6O_3Zn$: C, 65.65; H, 6.58; N, 11.21. Found: C, 64.99; H, 6.41; N, 11.61.

$L'Zn-OCOOEt$ (5b). This was prepared like **5a** with 20 mL of ethanol: yield 190 mg (86%) of colorless **5b**; mp 253 °C dec; $\nu(BH)$ 2550 cm^{-1} , $\nu(CO)$ 1713 and 1303 cm^{-1} . Anal. Calcd for $C_{42}H_{51}BN_6O_3Zn$: C, 66.02; H, 6.73; N, 11.00. Found: C, 65.75; H, 6.48; N, 11.37.

$L'Zn-SCOOEt$ (6). (a) **From CS₂.** A 200 mg (0.29 mmol) sample of **1** was dissolved in 30 mL of dichloromethane, and 20 mL of ethanol was added. After addition of 18 μ L (23 mg, 0.30 mmol) of CS_2 the solution was stirred for 5 h. Then all volatiles were removed in vacuo and the solid residue extracted three times with 3 mL of ethanol each. The remaining colorless solid (170 mg, 76%) consisted of 83% of **6** and 17% of **4** according to H-NMR. Repeated recrystallization from benzene/ethanol mixtures resulted in rather small amounts of a product consisting of **6** with only traces of **4**.

(b) **From KCS₂OEt.** A 200 mg (0.29 mmol) sample of **1** in 30 mL of dichloromethane was treated dropwise with stirring with a solution of 46 mg (0.29 mmol) of potassium xanthogenate in 20 mL of ethanol. After 1 h of stirring, the volume of the solution was reduced to one-half in vacuo. Then the solution was allowed to slowly evaporate in a nitrogen atmosphere to about 5 mL within a few days. A 199 mg (87%) yield of **6** precipitated, which was filtered off and dried in vacuo. **6** forms colorless crystals, mp 173 °C, $\nu(BH)$ 2553 cm^{-1} . Anal. Calcd for $C_{42}H_{51}BN_6OS_2Zn$: C, 62.84; H, 6.59; N, 9.83. Found: C, 63.36; H, 6.46; N, 10.55.

$(L'Zn)_2SO_3$ (7). A 200 mg (0.29 mmol) sample of **1** in 20 mL of dichloromethane was combined with 0.5 mL of methanol saturated with SO_2 . After 5 h of stirring, the solvents were removed in vacuo and the residue crystallized from acetonitrile. A 190 mg (92%) yield of **7**, mp 212 °C dec, $\nu(BH)$ 2541 cm^{-1} , $\nu(SO)$ 886 cm^{-1} , was obtained as colorless crystals. Anal. Calcd for $C_{78}H_{92}B_2N_{12}O_3SZn_2$: C, 65.51; H, 6.48; N, 11.72; Zn, 9.1. Found: C, 65.11; H, 6.43; N, 11.69; Zn, 10.5.

$L'Zn-SC(O)NHPH$ (8). A 200 mg (0.29 mmol) sample of **1** in 30 mL of dichloromethane was treated with 35 μ L (39 mg, 0.29 mmol) of phenyl isothiocyanate. After 2 h of stirring, the solvent was removed in vacuo and the residue taken up in a minimum amount of acetonitrile and crystallized at –30 °C. A 210 mg (88%) yield of **8** was obtained as colorless crystals, mp 144 °C, $\nu(BH)$ 2544 cm^{-1} , $\nu(CO)$ 1613 cm^{-1} .

(44) Förster, M.; Burth, R.; Powell, A. K.; Eiche, T.; Vahrenkamp, H. *Chem. Ber.* **1993**, *126*, 2643–2648.

(45) Elguero, J.; Jaquier, R. *Bull. Soc. Chim. Fr.* **1966**, 2832–2845.

(46) Baddeley, G.; Holt, G.; Pickless, W. *J. Chem. Soc.* **1952**, 4162–4166.

(47) Swamer, F. W.; Hauser, C. R. *J. Am. Chem. Soc.* **1950**, *72*, 1352–1356.

Table 1. Crystallographic Data^a

	1	2	2'	3'	4	5a	6
formula	C ₃₉ H ₄₇ BN ₆ OZn· CH ₃ OH	C ₃₉ H ₄₇ BN ₆ SZn	C ₃₉ H ₄₇ BN ₆ SZn· C ₆ H ₆	C ₇₈ H ₉₂ B ₂ N ₁₂ OZn ₂ · 2CH ₃ OH·H ₂ O	C ₇₈ H ₉₂ B ₂ N ₁₂ SZn ₂	C ₄₁ H ₄₉ BN ₆ O ₃ Zn	C ₄₂ H ₅₁ BN ₆ OS ₂ Zn
mol wt	724.05	708.07	786.17	1448.2	1382.06	750.04	796.19
space group	P2 ₁ /n	P1	P1	C2/c	P2 ₁ /n	P2 ₁ /n	P2 ₁ /n
Z	4	2	2	4	4	4	4
a (pm)	886.5(1)	1170.4(1)	1229.7(2)	2329.3(14)	2111.4(2)	879.4(5)	942.0(2)
b (pm)	2280.3(2)	1340.7(1)	1399.1(2)	1336.9(3)	1537.8(1)	2232.9(7)	2242.3(4)
c (pm)	1971.1(1)	1398.3(4)	1461.7(2)	2674.5(8)	2342.4(2)	2000.1(8)	2014.4(4)
α (deg)	90	74.83(1)	72.36(1)	90	90	90	90
β (deg)	93.46(1)	86.12(1)	65.31(1)	104.61(4)	105.23(1)	93.44(4)	92.90(3)
γ (deg)	90	70.50(1)	81.33(1)	90	90	90	90
V (nm ³)	3.9773(6)	1.9958(6)	2.1766(6)	8.059(6)	7.338(1)	3.920(3)	4.249(1)
d _{calc} (g cm ⁻³)	1.21	1.18	1.20	1.18	1.25	1.27	1.24
d _{obs} (g cm ⁻³)	1.20	1.20	1.20	1.20	1.26	1.25	1.21
$\bar{\mu}$ (mm ⁻¹)	0.658	0.701	0.649	0.649	0.733	0.672	0.715
R ₁ (obsd reflns)	0.062	0.070	0.069	0.079	0.070	0.048	0.041
wR ₂ (all reflns)	0.205	0.220	0.198	0.369	0.220	0.184	0.122

$$^a R_1 = \sum |F_o - F_c| / \sum F_o, wR_2 = [\sum [w(F_o^2 - F_c^2)^2] / \sum [w(F_o^2)^2]]^{1/2}.$$

Anal. Calcd for C₄₆H₅₂BN₇OSZn: C, 66.79; H, 6.34; N, 11.85. Found: C, 67.07; H, 6.57; N, 11.58.

¹H-NMR Data (CDCl₃, Internal TMS). KL: 1.20 [d, ³J = 6.9 Hz, 18H, Me(*i*-Pr)], 2.55 [s, 9H, Me(Pz)], 2.74 [spt, ³J = 6.9 Hz, 3H, H(*i*-Pr)], 6.20 [s, 3H, H(Pz)], 7.08 [d, ³J = 8.2 Hz, 6H, Cum(3,5)], 7.39 [d, ³J = 8.2 Hz, 6H, Cum(2,6)]. **1**: 1.27 [d, ³J = 6.9 Hz, 18H, Me(*i*-Pr)], 2.55 [s, 9H, Me(Pz)], 2.94 [spt, ³J = 6.9 Hz, 3H, H(*i*-Pr)], 6.28 [s, 3H, H(Pz)], 7.31 [d, ³J = 8.2 Hz, 6H, Cum(3,5)], 7.78 [d, ³J = 8.2 Hz, 6H, Cum(2,6)]. **2**: 1.27 [d, ³J = 6.9 Hz, 18H, Me(*i*-Pr)], 2.56 [s, 9H, Me(Pz)], 2.94 [spt, ³J = 6.9 Hz, 3H, H(*i*-Pr)], 6.19 [s, 3H, H(Pz)], 7.27 [d, ³J = 8.2 Hz, 6H, Cum(3,5)], 7.61 [d, ³J = 8.2 Hz, 6H, Cum(2,6)]. **3'**: 0.79 [d, ³J = 6.9 Hz, 24H, Me(*i*-Pr)], 1.36 [d, ³J = 6.9 Hz, 12H, Me(*i*-Pr)], 2.32 [s, 12H, Me(Pz)], 2.60 [spt, ³J = 6.9 Hz, 4H, H(*i*-Pr)], 2.63 [s, 6H, Me(Pz)], 3.05 [spt, ³J = 6.9 Hz, 2H, H(*i*-Pr)], 6.12 [s, 2H, H(Pz)], 6.26 [s, 4H, H(Pz)], 6.68 [d, ³J = 8.2 Hz, 8H, Cum(3,5)], 7.00 [d, ³J = 8.2 Hz, 8H, Cum(2,6)], 7.31 [d, ³J = 8.2 Hz, 4H, Cum(3,5)], 7.39 [d, ³J = 8.2 Hz, 4H, Cum(2,6)]. **4**: 0.74 [d, ³J = 6.9 Hz, 36H, Me(*i*-Pr)], 2.42 [spt, ³J = 6.9 Hz, 6H, H(*i*-Pr)], 2.55 [s, 18H, Me(Pz)], 6.20 [s, 6H, H(Pz)], 6.54 [d, ³J = 8.2 Hz, 12H, Cum(3,5)], 7.34 [d, ³J = 8.2 Hz, 12H, Cum(2,6)]. **5a**: 1.25 [d, ³J = 6.9 Hz, 18H, Me(*i*-Pr)], 2.42 [s, 3H, OMe], 2.53 [s, 9H, Me(Pz)], 2.92 [spt, ³J = 6.9 Hz, 3H, H(*i*-Pr)], 6.22 [s, 3H, H(Pz)], 7.28 [d, ³J = 8.2 Hz, 6H, Cum(3,5)], 7.57 [d, ³J = 8.2 Hz, 6H, Cum(2,6)]. **5b**: 0.40 [t, ³J = 7.0 Hz, 3H, OCCH₃], 1.29 [d, ³J = 6.9 Hz, 18H, Me(*i*-Pr)], 2.57 [s, 9H, Me(Pz)], 2.83 [q, ³J = 7.0 Hz, 2H, OCH₂], 2.97 [spt, ³J = 6.9 Hz, 3H, H(*i*-Pr)], 6.28 [s, 3H, H(Pz)], 7.31 [d, ³J = 8.2 Hz, 6H, Cum(3,5)], 7.61 [d, ³J = 8.2 Hz, 6H, Cum(2,6)]. **6**: 0.23 [t, ³J = 6.6 Hz, 3H, OCCH₃], 1.23 [d, ³J = 6.9 Hz, 18H, Me(*i*-Pr)], 2.54 [s, 9H, Me(Pz)], 2.78 [q, ³J = 6.6 Hz, 2H, OCH₂], 2.89 [spt, ³J = 6.9 Hz, 3H, H(*i*-Pr)], 6.17 [s, 3H, H(Pz)], 7.24 [d, ³J = 8.2 Hz, 6H, Cum(3,5)], 7.54 [d, ³J = 8.2 Hz, 6H, Cum(2,6)]. **7**: 0.80 [d, ³J = 6.9 Hz, 36H, Me(*i*-Pr)], 2.46 [spt, ³J = 6.9 Hz, 6H, H(*i*-Pr)], 2.53 [s, 18H, Me(Pz)], 6.18 [s, 6H, H(Pz)], 6.60 [d, ³J = 8.2 Hz, 12H, Cum(3,5)], 7.45 [d, ³J = 8.2 Hz, 12H, Cum(2,6)]. **8**: 1.21 [d, ³J = 6.9 Hz, 18H, Me(*i*-Pr)], 2.54 [s, 9H, Me(Pz)], 2.87 [spt, ³J = 6.9 Hz, 3H, H(*i*-Pr)], 6.15 [s, 3H,

H(Pz)], 6.83–6.97 [m, 5H, NPh], 7.18 [d, ³J = 8.2 Hz, 6H, Cum(3,5)], 7.54 [d, ³J = 8.2 Hz, 6H, Cum(2,6)].

¹³C-NMR Data (CDCl₃, Internal TMS). KL: δ = 12.6 (pz–Me), 24.0 (*i*-PrMe), 33.7 (*i*-Pr-CH), 102.2, 125.3, 126.6, 133.4 (aromatic), 145.3, 147.1, 150.3 (pyrazole). **1**: δ = 12.9 (pz–Me), 23.8 (*i*-PrMe), 33.9 (*i*-Pr-CH), 104.3, 126.8, 127.3, 129.1 (aromatic), 145.6, 149.3, 153.2 (pyrazole). The ¹³C-NMR data of complexes **2–8** differ only little from those of **1**.

X-ray Crystallography. Crystals were obtained either directly from the reaction solutions or by slow evaporation from the solvents given in Table 1. Diffraction data were recorded at room temperature (at –100 °C for **5a**) with the ω/2θ technique on a Nonius CAD4 diffractometer fitted with a molybdenum tube (Kα, λ = 0.7107 Å) and a graphite monochromator. An absorption correction (program DI-FABS⁴⁸) was only applied to **5a**. The structures were solved with direct methods and refined anisotropically with the SHELX program suite.⁴⁹ Hydrogen atoms were included with fixed distances and isotropic temperature factors 1.2 times those of their attached atoms (1.5 times in methyl groups). Some cocrystallized solvent molecules were found for **2'** and **3'** which are not connected to the complexes, while the cocrystallized methanol in **1** is hydrogen bonded to the Zn–OH group. Parameters were refined against F². Drawings were produced with SCHAKAL.⁵⁰ Table 1 lists the crystallographic data.

Supporting Information Available: Fully labeled ORTEP plots and listings of crystal data, bond distances and angles, anisotropic thermal parameters, and hydrogen positions for **1**, **2**, **2'**, **5a**, and **6** (31 pages). Ordering information is given on any current masthead page. The structures of **3'** and **4** have already been documented.¹³

IC960335A

(48) Walker, N.; Stuart, D. *Acta Crystallogr., Part A* **1983**, *39*, 158–166.

(49) Sheldrick, G. M. SHELXS and SHELXL, Programs for Crystal Structure Determination. Göttingen, Germany, 1986 and 1993.

(50) Keller, E. SCHAKAL-93. Freiburg, Germany, 1993.